

Mechanochemical Aspects of Axonemal Dynein Activity Studied by In Vitro Microtubule Translocation

T. Hamasaki,* M. E. J. Holwill,‡ K. Barkalow,* and P. Satir*

*Department of Anatomy and Structural Biology, Albert Einstein College of Medicine, Bronx, New York 10461 USA, and ‡Department of Physics, Kings College, London, England

ABSTRACT We have determined the relationship between microtubule length and translocation velocity from recordings of bovine brain microtubules translocating over a *Paramecium* 22S dynein substratum in an in vitro assay chamber. For comparison with untreated samples, the 22S dynein has been subjected to detergent and/or to pretreatments that induce phosphorylation of an associated 29 kDa light chain. Control and treated dyneins have been used at the same densities in the translocation assays. In any given condition, translocation velocity (v) shows an initial increase with microtubule length (L) and then reaches a plateau. This situation may be represented by a hyperbola of the general form $v = aL/(L + b)$, which is formally analogous to the Briggs-Haldane relationship, which we have used to interpret our data. The results indicate that the maximum translocation velocity $v_0 (= a)$ is increased by pretreatment, whereas the length constant $K_L (= b)$, which corresponds to K_m , does not change with pretreatment, implying that the mechanochemical properties of the pretreated dyneins differ from those of control dyneins. The conclusion that K_L is constant for defined in vitro assays rules out the possibility that the velocity changes seen are caused by changes in geometry in the translocation assays or by the numbers of dyneins or dynein heads needed to produce maximal translocational velocity. From our analysis, we determine that f , the fraction of cycle time during which the dynein is in the force-generating state, is small—roughly 0.01, comparable to the f determined previously for heavy meromyosin. The practical limits of these mechanochemical changes imply that the maximum possible ciliary beat frequency is about 120 Hz, and that in the physiological range of 5–60 Hz, beat frequency could be controlled by varying the numbers of phosphorylated outer arm dyneins along an axonemal microtubule.

INTRODUCTION

In a series of studies (Hamasaki et al., 1991; Barkalow et al., 1994b), we have measured the velocity of microtubule translocation by 22S dynein from *Paramecium tetraurelia* in in vitro assays (Vale and Toyoshima, 1988) after a number of treatments designed to alter translocation velocity. Such treatments include phosphorylation—either in situ by pretreatment of axonemes in the presence of cAMP and ATP or γ S-ATP or in vitro by treating the isolated 22S dynein with a *Paramecium* protein kinase A (PKA)—and/or detergent addition (Vale and Toyoshima, 1989). In the living cilium, provided there are no changes in beat form, the velocity of microtubule sliding is directly proportional to the frequency of beat (Satir et al., 1993). The increase in microtubule translocation velocity in the in vitro assays provides a relevant model for physiological increases in beat frequency in a second messenger cascade. In support of this as a reasonable model is the fact that phosphorylation of a 29-kDa dynein regulatory light chain (p29) increases both translocation velocity in vitro and the swimming speed of permeabilized cells (Hamasaki et al., 1991); the increase in swimming speed probably reflects an increase in the ciliary beat frequency. In the previous papers, the average

velocities of the microtubules were presented. We have now reexamined the data to measure the velocities as a function of length, and we report here a rigorous analysis of the clear asymptotic pattern that emerges.

The mechanism by which microtubule translocation velocity is increased by phosphorylation is not yet clear, although obviously it depends on the mechanochemical properties of the 22S dynein itself and the susceptibility of these properties to change. Comparable problems exist in the two other in vitro motility systems that have been developed: the movement of actin microfilaments on isolated myosin or its subfragments (Uyeda et al., 1990; Harada et al., 1990; Yanagida et al., 1993; Harris and Warshaw, 1993) and microtubule translocation by kinesin (Block et al., 1990; Vale et al., 1992; Howard et al., 1989). All indications are that the dynein and myosin systems resemble one another in several important features and that they differ in those features from kinesin. Hydrolysis of ATP by one molecule of any of these motors provides a force of about 6–7 pN, sufficient to move a 10- μ m-long microtubule. This force can be measured directly for kinesin-induced microtubule translocation (Svodoba et al., 1993; Hunt et al., 1994) and for myosin (Finer et al., 1994). For kinesin, the duty phase (the time (t_s) of strong attachment to the microtubule) is a large fraction (f), perhaps 80% or more, of its total cycle time (t_c), where

$$f = t_s/t_c. \quad (1)$$

The values of f for both myosin and dynein are probably much smaller than that for kinesin, and, even though one

Received for publication 2 December 1994 in final form 4 September 1995.

Address reprint requests to Dr. Peter Satir, Department of Anatomy and Structural Biology, Albert Einstein College of Medicine, Bronx, NY 10461. Tel.: 718-430-4061; Fax: 718-430-8996; E-mail: satir@aecom.yu.edu.

© 1995 by the Biophysical Society
0006-3495/95/12/2569/11 \$2.00

molecule is sufficient to produce the force necessary for translocation, many molecules are necessary to produce the actual motion. Under normal in vitro conditions, the translocating organelle will not stay in place without continuous attachment to the motor, and a single cycling molecule cannot maintain continuous strong attachment to the organelle. For dynein, Vale et al. (1992) calculate, on the basis of average force production, that around 10 dynein molecules are the equivalent of one kinesin in such assays. The value of f for dynein is therefore likely to be about an order of magnitude smaller than 0.8, comparable with the values determined for myosin. Uyeda et al. (1990) have used the equation

$$v = v_o\{1 - (1 - f)^N\} \quad (2)$$

to estimate f for myosin heavy mero-myosin fragments (HMM), where v_o is the velocity at which a motor moves during its duty phase, N is the average number of heads that interact with the filament, and v is the experimentally determined translocation velocity for the filament. From measurements of translocation velocities for filaments of varying lengths at differing motor densities, Uyeda et al. (1990) calculate that $f = 0.05$ for HMM. Comparable values have been determined by Harris and Warshaw (1993).

In this study, we have taken a different approach to determining cycle parameters for *Paramecium* 22S dynein, with a view to learning how they might be changed on phosphorylation. We have determined the relationship between microtubule length and translocation velocity for the microtubules studied previously, with different pretreatments of the 22S dynein over which the microtubules move, but with control and treated dyneins used at the same density in the translocation assays. As with myosin in any given condition, the velocity at first increases with microtubule length and then reaches a plateau. This pattern of behavior is characteristic of a hyperbolic function, analogous to Briggs-Haldane kinetics. We have used the analogous constants derived from the best-fit hyperbolas to interpret our data; in this way, we determine parameters associated with the dynein-tubulin interaction and assess their significance with respect to the mechanochemistry of the system.

One particular difficulty in understanding how dynein works in the translocation experiments is the small number of molecules that need to be affected to cause an increase in the translocation velocity. Hamasaki et al. (1991) have determined that only a small percentage (2–10%) of 22S dynein needs to show increased phosphorylation to produce a 40% increase in microtubule translocation velocity. This is further confirmed in the reconstitution experiments, where only a few phosphorylated p29 chains when recombined with untreated 22S dynein are able to translocate microtubules significantly faster than controls (Barkalov et al., 1994b). The analysis of the mechanochemical parameters of dynein-based microtubule translocation developed in this paper provides an insight into this puzzling result.

KINETIC THEORY

Assume that the conditions under which movement occurs are such that when an individual dynein arm strongly interacts with a microtubule, the distance through which the microtubule is driven depends on the step size of the mechanochemical cycle of the arm, but is in the first instance independent of the length of the microtubule. In general, “dead heads” (i.e., dynein molecules that attach strongly to the microtubule and do not release in the presence of ATP) do not seem to impede this process significantly. Although we have not measured the number of dead heads directly in these experiments, in earlier preparations it could be shown that virtually 100% of the dynein arms that decorate microtubules are released by 0.1–1 mM ATP (Satir et al., 1981). For a given concentration of dynein arms arranged randomly on a substratum, the number that potentially could interact with a given microtubule is proportional to the length of that microtubule.

In general, in the assays we employ, an individual microtubule will be translocated by many dynein arms. We assume that the arms cycle with random phases in such a way that they do not interfere with each other during the strong attachment phase and that where the strong attachment phases of two different arms coincide exactly, the distance through which they propel the microtubule is one step size rather than two. Where there is an overlap rather than coincidence, the distance moved is reduced in proportion to the overlap. These assumptions are consistent with movement occurring under essentially unloaded conditions.

As the length of microtubule increases, so also will the number of strongly interacting dynein arms. The velocity at which the microtubule moves is determined by the number of noncoincident strong attachment phases, which (unless $f = 1$) must also increase with the length (L) of the microtubule. This increase in velocity of translocation will continue until the numbers of dyneins interacting with the microtubule are such that at least one arm is always in the strong attachment phase of its cycle, after which the velocity of translocation, now maximized, will become independent of further increase in microtubule length. This velocity can be represented by a constant (v_o). This situation may be represented graphically by a hyperbola of the general form:

$$v = aL/(L + b). \quad (3)$$

This equation and the underlying assumptions are formally analogous to the Briggs-Haldane (1925) relationship, which describes the rate V of an enzymatic reaction

$$\frac{V}{V_{\max}} = \frac{[S]}{[S] + K_m}, \quad (4)$$

and are not substantially different from the analysis of Uyeda et al. (1990).

In Eq. 4, V_{\max} is the maximum rate of the reaction, $[S]$ represents substrate concentration, and K_m is the Michaelis-Menten constant, corresponding to the substrate concentra-

tion for half-maximum velocity. Earlier studies (e.g., Brokaw, 1967) have shown that the beat frequency of demembrated cilia is proportional to V . Under conditions where the bend shape is unaltered, beat frequency is proportional to microtubule sliding velocity (e.g., Satir et al., 1993); the microtubule sliding velocity is therefore proportional to the enzyme reaction rate. The *in vitro* sliding preparations used in this study rely on the same kinetic mechanism as that in the bending cilium, and it is therefore reasonable to expect the sliding rate here also to be proportional to the velocity of some element of the dynein-tubulin mechanochemical cycle. Specifically, we consider the velocity to be proportional to the rate of product formation from the D-ADP- P_i complex (where D represents dynein) that probably represents the beginning of the strong attachment phase of the arm cycle (Johnson, 1985). Our analysis suggests that, in a simplified way, the breakdown of this complex, accelerated enzymatically by attachment to the overlying microtubule, can be thought of as the kinetic step of substrate to product breakdown, whose rate of reaction is responsible for the velocity of microtubule translocation.

If v and v_o are the microtubule translocation velocities corresponding to V and V_{max} , the Briggs-Haldane relationship (Eq. 4) can be rewritten:

$$\frac{v}{v_o} = \frac{L}{L + K_L} \quad (5)$$

where K_L is the microtubule length necessary for half-maximal velocity, analogous to the Michaelis-Menten constant. Rearranging this equation in the manner suggested by Lineweaver and Burk (1934) we obtain

$$\frac{1}{v} = \frac{1}{v_o} + \frac{K_L}{v_o L} \quad (6)$$

As will be seen, plots of $1/v$ against $1/L$ are essentially linear, supporting our argument for the determination of v_o and K_L , the significance of which will be discussed later. Because N , the average number of heads that interact with a microtubule, is a function of motor density on the substratum, which can be determined experimentally, N can be calculated for any microtubule length. Hence, using the experimentally calculated value of N for a microtubule of length K_L , together with Eqs. 1 and 2, f can be determined and the relation of step size d ($= v_o t_s$) to cycle time (t_c) can be estimated for any pretreatments with minimal further assumptions.

Within certain limits to be discussed, our results permit us to rule out the possibility that the velocity changes seen upon phosphorylation and/or detergent treatment are caused by changes in geometry or by the numbers of dynein heads needed to produce translocational maximal velocity.

MATERIALS AND METHODS

Experimental basis

Data comparing lengths of individual microtubules with their translocation velocities have been collected from videotape records of experiments previously reported by Hamasaki et al. (1991) and Barkalow et al. (1994b). Briefly, these experiments utilized isolated 22S *Paramecium tetraurelia* dynein on a glass substratum, and Taxol-stabilized brain microtubules, polymerized from phosphocellulose-purified twice-recycled tubulin, in the presence of 1 mM ATP (K_m for sliding microtubules is 210 μ M; Oiwa and Takahashi, 1988) at room temperature. Comparable aliquots of control versus experimentally pretreated 22S dyneins were used. Some pretreatments were performed on isolated axonemes. The axonemes were incubated with 10–100 μ M γ S-ATP in the presence or absence of 20 μ M cAMP with or without 10^{-4} M Ca^{2+} . Other treatments were on isolated 22S dynein itself, and these included addition of 10 μ M cAMP with or without $\sim 10U$ *Paramecium* PKA (Walczak et al., 1994; Barkalow et al., 1994) together with 1 mM ATP to phosphorylate the dynein. In these experiments, the same dynein substratum was used before and after addition of PKA. In some experiments, the 22S dynein substratum was perfused with 0.1% Triton X-100 (Pierce Science, IL), together with Mg^{2+} -ATP, for 3 min. Records were taken in darkfield with a Zeiss standard microscope (Zeiss, NY) equipped with a Hamamatsu SIT camera (Hamamatsu, Japan). Images of moving microtubules were tracked for up to 30 s, and translocation velocities were calculated from distance moved divided by time, using the microtubule centroids to establish initial and final positions for 2- or 4-s samples during the continuous movement. For some microtubules, measurements were taken at both 2 and 4 s, and the average of the two measurements was used. Microtubules that stopped or noticeably changed speed during the 30 s of monitoring were not used.

Data analysis

In any given condition, translocation velocities for many individual microtubules (Fig. 1) can be plotted against microtubule length. Using the Levenberg-Marquardt algorithm (Press et al., 1992) in a DeltaGraph Pro 3.5 for Windows software package (DeltaPoint Co.), we have fitted the optimal hyperbola described by Eq. 3 to each data set. We have also used SigmaPlot for Windows version 2.0 (Jandel Scientific Corp.). In each case tested, the values for a and b converge on a particular solution. These values, corresponding to v_o and K_L , respectively, have been used to plot straight lines through the data graphed as $1/v$ versus $1/L$ according to Eq. 6, analogous to the Lineweaver-Burk relationship, as shown in Figs. 1–3. To simplify the presentation of data, lengths of microtubules were also pooled arbitrarily in bins, and the average length and average velocity of each bin were calculated. Two different bin ranges have been tested. In consolidation method I, bins are of equal size: 1–2 μ m; 2–3 μ m, etc. In consolidation method II, bins increase in size as microtubule length increases to keep the numbers of measurements per bin comparable: 1–2 μ m, 2–3 μ m, etc.; 10–12 μ m, etc.; 14–17 μ m, etc.; 20–25 μ m, etc.; 30–40 μ m, etc. Although the individual data sets differ, there are no obvious changes in overall outcome when the alternative consolidation methods are used, and both consolidation methods yield virtually the same hyperbolic curves as the nonconsolidated data set (Fig. 1). Furthermore, the χ -square analysis using the data sets is quite robust. The values of v_o and K_L derived from the various hyperbolas \pm asymptotic standard errors (obtained with SigmaPlot) are given in Tables 1–3.

Determination of dynein density

The density of dynein in the translocation chamber was determined directly by counting individual dynein molecules in several separate fields, seen in negative-stain electron micrographs taken of grids to which the dynein was applied in the same manner as in the corresponding translocation chambers, as detailed in Hamasaki et al. (1991). For electron microscopic methods, see Barkalow et al. (1994a).

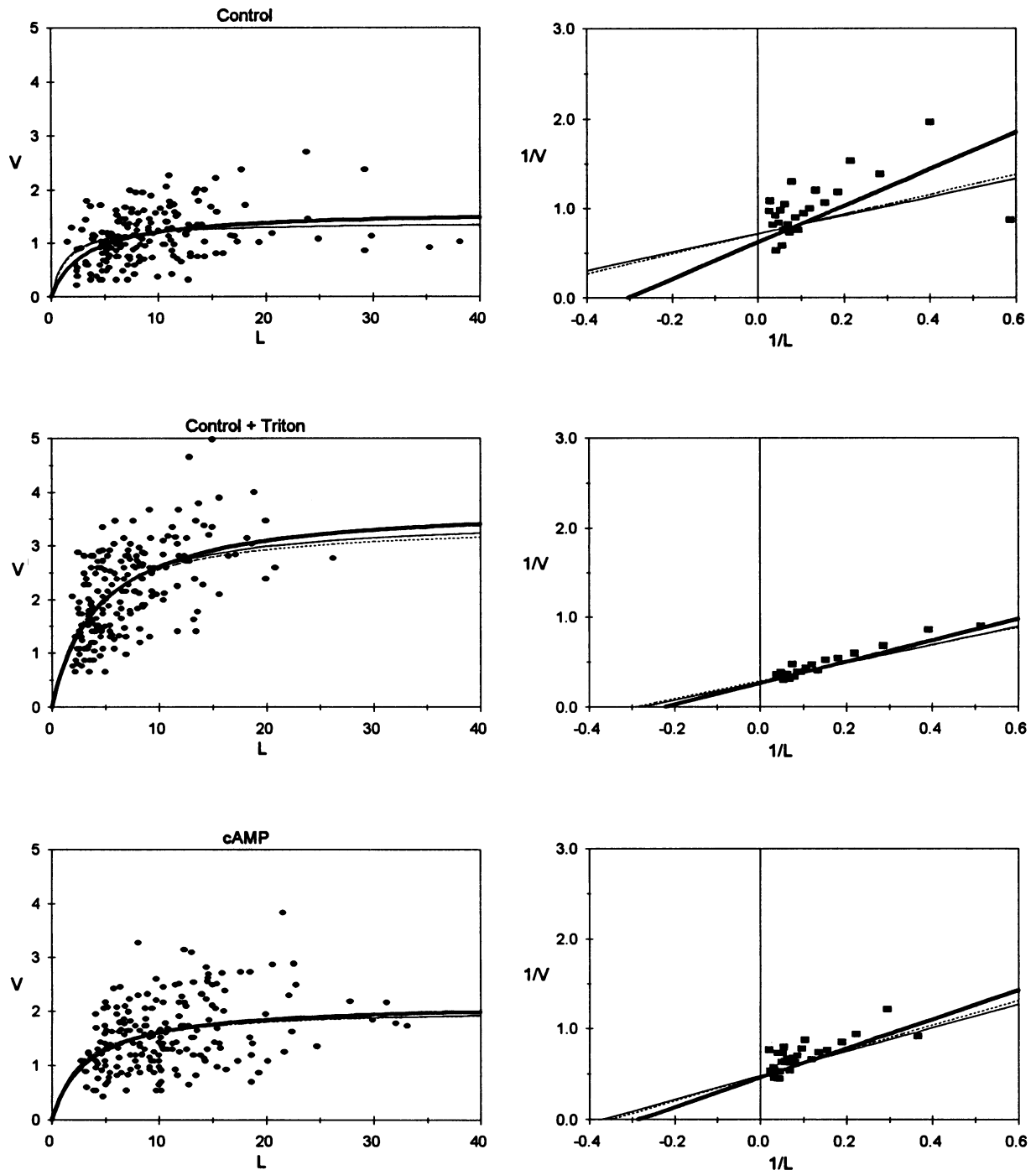


FIGURE 1 (a) Determination of v_0 and K_L by the Levenberg-Marquardt algorithm. The graphs show a typical data set to which optimal hyperbolas described by Eq. 3 have been fitted, so that values of a and b , representing v_0 and K_L , respectively, can be determined. The hyperbolas derived from data sets from consolidation methods I and II are also indicated in each instance. For the nonconsolidated data sets shown: control: χ^2 converges to 34.0 ($n = 183$); control + Triton: χ^2 converges to 83.2 ($n = 205$); cAMP: χ^2 converges to 66.9 ($n = 204$). (b) Plots of $1/v$ versus $1/L$ for the data sets from the Levenberg-Marquardt-derived hyperbolas shown in *a*. The lines are drawn using the values from each hyperbola. The squares are data points from consolidated method I for visualization of fit. Note that $-1/K_L$ is approximately constant in all cases. Thick lines: nonconsolidated data set. Thin and dotted lines: consolidated data sets I and II, respectively.

RESULTS

Although each microtubule normally moves at a characteristic velocity for 20–30 s across the dynein substratum,

images with a time resolution of 100 ms show momentary variations of about $\pm 50\%$ around a mean. Individual microtubules of the same length have somewhat different characteristic velocities, which might reflect inhomogeneity

TABLE 1 Determination v_o and K_L in translocation experiments with 22S dynein after various pretreatments*

Condition	v_o			K_L			Recalc. v_o^{\ddagger}	$N(K_L)^{\S}$	f
	NC	I	II	NC	I	II			
Control	1.6 ± 0.1	1.4 ± 0.1	1.4 ± 0.1	3.3 ± 0.9	1.4 ± 0.9	1.6 ± 0.7	1.7 ± 0.05	49	0.014
cAMP	2.2 ± 0.2	2.1 ± 0.1	2.1 ± 0.1	3.5 ± 0.9	2.7 ± 0.9	2.9 ± 0.8	2.3 ± 0.06	52	0.013
cAMP, pCa4	1.9 ± 0.2	1.8 ± 0.2	1.8 ± 0.2	6.5 ± 1.8	5.6 ± 2.3	6.3 ± 1.8	1.6 ± 0.05	97	0.007
Control + Triton	3.8 ± 0.2	3.5 ± 0.2	3.4 ± 0.2	4.5 ± 0.7	3.6 ± 0.8	3.4 ± 0.6	3.7 ± 0.07	67	0.010
cAMP + Triton	3.6 ± 0.2	3.5 ± 0.3	3.6 ± 0.2	3.2 ± 0.6	2.9 ± 1.0	3.0 ± 0.6	3.9 ± 0.09	48	0.014
cAMP, pCa4 + Triton	3.0 ± 0.2	3.1 ± 0.3	3.2 ± 0.3	3.3 ± 0.7	3.3 ± 1.4	3.8 ± 1.1	3.2 ± 0.08	50	0.014

*See Hamasaki et al. (1991) for pretreatment conditions; values of v_o and K_L for each condition calculated as in Fig. 1 a. NC, nonconsolidated data. I and II, data after application of consolidation methods I and II, respectively.

$\ddagger K_L = 4.1$ average from nonconsolidated data.

$\S N(K_L)$ from nonconsolidated data; see Eq. 7 for calculation of f .

of the substratum or the stochastic nature of the stepping process. Microtubules of different lengths moving across similar, but perhaps nonidentical, parts of the field, either at the same time or in procession, often have different velocities. For these reasons, plots of microtubule velocity (v) against microtubule length (L) show considerable scatter (Fig. 1 a), but there is a clear tendency for the velocity to increase with length before reaching a plateau. This tendency is observed in all the preparations examined, irrespective of the dynein pretreatment, but is most apparent in those with the fastest translocation velocities.

In each case shown in Fig. 1 a, the data can readily be fitted with a hyperbola derived by the Levenberg-Marquardt method, whose constants, v_o and K_L , are given in Table 1. It is evident in Fig. 1 that the hyperbolas derived from either consolidated data set are virtually identical to the hyperbola derived from the nonconsolidated data. To aid in visualization, we have plotted the consolidated data from averaging method I in the form $1/v$ versus $1/L$ (Fig. 1 b), which will produce a linear relationship, analogous to a Lineweaver-Burk plot. The K_L and v_o values used to draw the lines relating to the various dynein pretreatments in Fig. 1 b have been determined from the appropriate hyperbolas. The slopes of the lines are different, and are such as to confirm that, at all values of microtubule length measured, the cAMP-pretreated and detergent-treated dyneins translocate microtubules faster than the controls. The maximum velocities (v_o , Table 1) are also different. Table 1 records the values of v_o and K_L for the unconsolidated data, and for the two consolidation methods we have employed. The small variations in the values of the parameters determined for a

given pretreatment reflect the different averaging procedures inherent in each method. An "average K_L " will be discussed below.

Selected experiments with cAMP and Triton were repeated using a different dynein preparation, which translocated microtubules faster than the initial preparations. The values for v_o and K_L obtained from these experiments are shown in Table 2. In addition, we have obtained values of v_o and K_L (Table 3), using the data from experiments where the 22S dynein was treated, after isolation, with 10 μ M cAMP and reactivated before (control) and then after addition of PKA (see also Barkalow et al., 1994b). Lineweaver-Burk-type plots of these experiments based on values of v_o and K_L determined by the optimal Levenberg-Marquardt hyperbolas are shown in Fig. 2.

Determination of average K_L and v_o^x

Inspection of Table 1 shows that the values of K_L obtained for the various pretreatment conditions are the same, within experimental error, suggesting that K_L may be a constant for the system. This seems likely because the preparations from which all the data were derived were made to give essentially the same surface concentration of dynein on the glass slide. To test this possibility, we calculated the average value for K_L from the nonconsolidated data, as shown in Table 1. We obtained a mean K_L of $4.1 \pm 1.2 \mu$ m. Using the new average K_L , we then constructed new Levenberg-Marquardt hyperbolas to determine new v_o values for each pretreatment (Recalculated v_o , Tables 1–3). The negative

TABLE 2 Determination v_o and K_L in translocation experiments with alternate 22S dynein after various pretreatments

Condition	v_o			K_L			Recalc. v_o^*	$N(K_L)^{\ddagger}$	f
	NC	I	II	NC	I	II			
Control	5.1 ± 0.9	5.5 ± 1.4	5.3 ± 1.3	7.8 ± 2.7	8.6 ± 5.0	8.2 ± 4.6	3.8 ± 0.14	116	0.006
cAMP	4.8 ± 0.6	4.7 ± 0.6	5.3 ± 0.8	3.2 ± 1.3	2.6 ± 1.3	3.5 ± 1.6	5.2 ± 0.20	47	0.015
Control + Triton	6.8 ± 0.5	8.0 ± 0.8	8.8 ± 0.8	6.0 ± 1.1	8.1 ± 2.2	9.9 ± 2.2	5.9 ± 0.15	88	0.008
cAMP + Triton	7.1 ± 0.5	8.3 ± 0.7	8.4 ± 0.9	3.9 ± 0.8	6.0 ± 1.5	6.1 ± 1.6	7.2 ± 0.16	57	0.012

* $K_L = 4.1$ (average from Table 1).

$\ddagger N(K_L)$ from nonconsolidated data; see Eq. 7 for calculation of f .

TABLE 3 Determination v_o and K_L in translocation experiments with control vs. PKA-treated 22S dynein

Condition	v_o			K_L			Recalc. v_o^\dagger	$N(K_L)^\S$	f
	NC	I	II	NC	I	II			
Control*	2.4 ± 0.8	2.1 ± 0.9	2.2 ± 0.9	3.4 ± 3.5	2.0 ± 4.6	1.9 ± 4.5	2.5 ± 0.22	50	0.014
PKA	3.7 ± 0.6	3.3 ± 0.4	3.4 ± 0.5	3.7 ± 2.0	3.0 ± 1.6	3.0 ± 1.6	3.8 ± 0.22	55	0.013

*Dynein treated with $10 \mu\text{M}$ cAMP and 1 mM ATP in the absence of added PKA.

$^\dagger K_L = 4.1$ (average from Table 1).

$^\S N(K_L)$ from nonconsolidated data; see Eq. 7 for calculation of f .

reciprocal of the average K_L value [-0.24] was then used as a fixed point together with the recalculated v_o values to generate new Lineweaver-Burk-type plots for all the pretreatment conditions. These are shown in Fig. 3, *a-c*; the relevant lines are as good a visual fit to the data as were the previous plots (Fig. 1 *b*). The calculated variances for the new hyperbolas are identical to those of the original hyperbolas ($\pm 1\%$ SD).

A similar situation obtains for the other data sets. When we replotted these data sets in Lineweaver-Burk form using the same average K_L [of $4.1 \mu\text{m}$] that we obtained above

and the corresponding recalculated v_o values, the fits of the new lines to the data sets were again as good as the fits of the lines drawn previously.

Weighting Tables 1–3 equally, with the assumption that PKA addition reproduces the cAMP-dependent phosphorylation seen in the other experiments, we have also calculated an average value of v_o for each given pretreatment condition. We list this value as v_o^\times in Table 4.

Determination of N for a microtubule of length K_L

A dynein field prepared in parallel to the translocation chamber substrata is shown in Fig. 4. Counts of 78 such fields from 3 preparations yield a value of 62 ± 23 molecules per $0.1 \mu\text{m}^2$ or ~ 620 molecules μm^{-2} . The molecules are randomly placed bouquets that occupy triangular-shaped areas of $\sim 1 \times 10^{-3} \mu\text{m}^2$ each (Barkalow et al., 1994a; base and height of triangle, 39 nm and 45 nm, respectively). Therefore, about 62% of the field over which the microtubules translocate is covered by the 22S dynein molecules. Accordingly, a microtubule $1 \mu\text{m}$ long and 24 nm wide placed on this field will touch about 15 different dynein molecules ($1-2$ per $0.1 \mu\text{m}$ length). Traveling for 10 s at a velocity of $1 \mu\text{m s}^{-1}$, the microtubule will move over about 165 molecules.

From the previous section, K_L is $4.1 \mu\text{m}$, a constant for our translocation experiments. A microtubule $4.1 \mu\text{m}$ long will be in contact with 60 dyneins. Therefore, if we assume that every dynein that touches a microtubule is capable of interacting with it to cause sliding, when $K_L = 4.1$, $N(K_L) = 60$, where $N(K_L)$ is the number of dynein molecules in contact with a microtubule of length K_L . In Tables 1–3, the range of $N(K_L)$ values from 47 to 116 is consistent with the standard error of K_L . The variation of $N(K_L)$ does not depend on the pretreatment to which the dynein was subjected; for example, control dynein preparations range from 49 to 116.

Determination of f

By definition, K_L is the microtubule length where $v = 0.5 v_o$. Therefore, from Eq. 2,

$$0.5 = (1 - f)^{N(K_L)}, \quad (7)$$

f can be calculated for any value of K_L and values are shown in Tables 1–3. In all cases, f approximates 0.01.

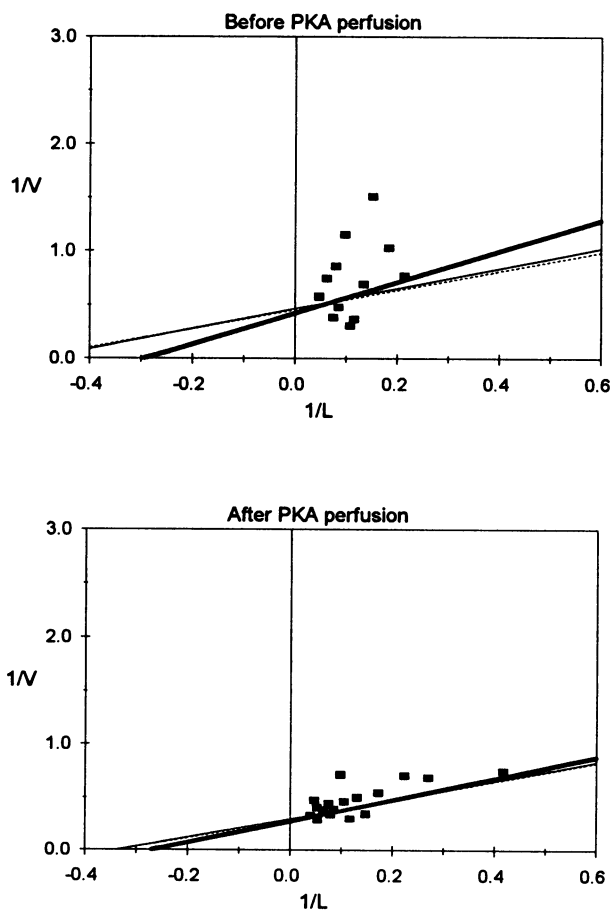


FIGURE 2 Plots of $1/v$ versus $1/L$ for a PKA experiment. Data points are from consolidation method I. Thick line shows fits from Levenberg-Marquardt-derived hyperbolas for nonconsolidated data (before PKA $\chi^2 = 16.0$, $n = 29$; after $\chi^2 = 40.9$, $n = 44$). Lines from consolidation methods I and II (thin line, broken line) are identical.

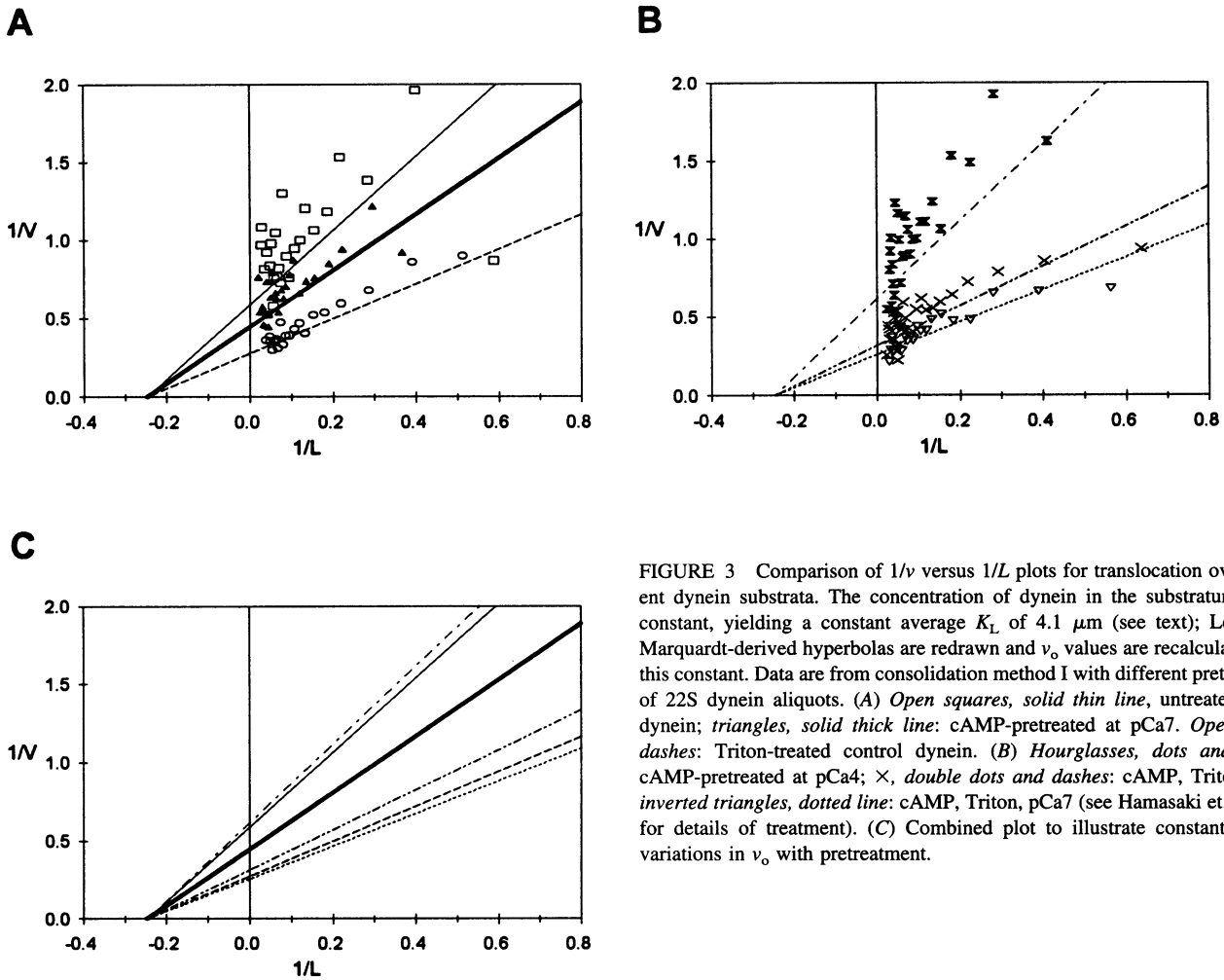


FIGURE 3 Comparison of $1/v$ versus $1/L$ plots for translocation over different dynein substrata. The concentration of dynein in the substratum is held constant, yielding a constant average K_L of $4.1 \mu\text{m}$ (see text); Levenberg-Marquardt-derived hyperbolas are redrawn and v_0 values are recalculated using this constant. Data are from consolidation method I with different pretreatments of 22S dynein aliquots. (A) *Open squares, solid thin line*, untreated control dynein; *triangles, solid thick line*: cAMP-pretreated at pCa7. *Open circles, dashes*: Triton-treated control dynein. (B) *Hourglasses, dots and dashes*, cAMP-pretreated at pCa4; *×*, *double dots and dashes*: cAMP, Triton, pCa4; *inverted triangles, dotted line*: cAMP, Triton, pCa7 (see Hamasaki et al., 1991, for details of treatment). (C) Combined plot to illustrate constant K_L with variations in v_0 with pretreatment.

DISCUSSION

Significance of K_L

In our analysis of microtubule sliding velocities, K_L is the microtubule length corresponding to half-maximal translocation velocity, and as such reflects aspects of the mechanochemical interaction between dynein and tubulin. In particular, through Eq. 7, it provides a measure of f , the fraction of the dynein molecule cycle time for which the dynein is strongly attached to tubulin, i.e., the force-generating state. Our results are consistent with a constant value for K_L , within the limits of experimental error, which suggests that f remains constant for different pretreatment conditions. The experimental error is, however, relatively large, and it is possible that the spread in the values of K_L reflects a true variation in this parameter. If the variation corresponds to the range of K_L observed, i.e., from about $1.4 \mu\text{m}$ to $9.9 \mu\text{m}$, $N(K_L)$ will vary from about 21 to 146, and f from .03 to .005. To raise f even to 0.2, K_L would have to be about $0.2 \mu\text{m}$, nearly an order of magnitude lower than our minimum value. Although the possible variation in f would have important consequences for force generation and the exact nature of mechanochemical events in the dynein arm

cycle, we can conclude that f for 22S dynein resembles that estimated for HMM, but is quite different from that for kinesin. This is consistent with earlier expectations (Vale et al., 1992). Because short microtubules do not regularly separate from the underlying dynein substratum, this con-

TABLE 4 Relationship between maximal sliding velocity (v_0^*) and ciliary beat frequency (H) for various 22S dyneins

Treatment*	v_0^*	t_E^*	H (Hz)
Control	2.7	37	6.7
cAMP/PKA	3.8	26	9.4
Triton	4.8	21	12.0
cAMP + Triton	5.6	18	13.9
All pp29 [‡]	13.7	7.3	34.3
V_{max}^{\S}	19	5.3	47.5
$d/t_c \text{ max}^{\parallel}$	48.5	2.1	121
All pp29	57.4	1.7	143

* v_0^* = Average values for various conditions from recalculated v_0 values in Tables 1-3 in $\mu\text{m s}^{-1}$; $t_E \approx 100 \text{ nm}/v_0^*$ (in ms); $v_0^* \approx 0.4 H$.

[‡]Takahashi et al. (1982).

[§] $d/t_c \text{ max} = 1/33 = f v_0^*$

[‡] v_0^* calculated on the basis of 10% pp29 in cAMP-treated dynein. See text.

^{||} v_0^* calculated on the basis of 2% pp29 in cAMP-treated dynein. See text.

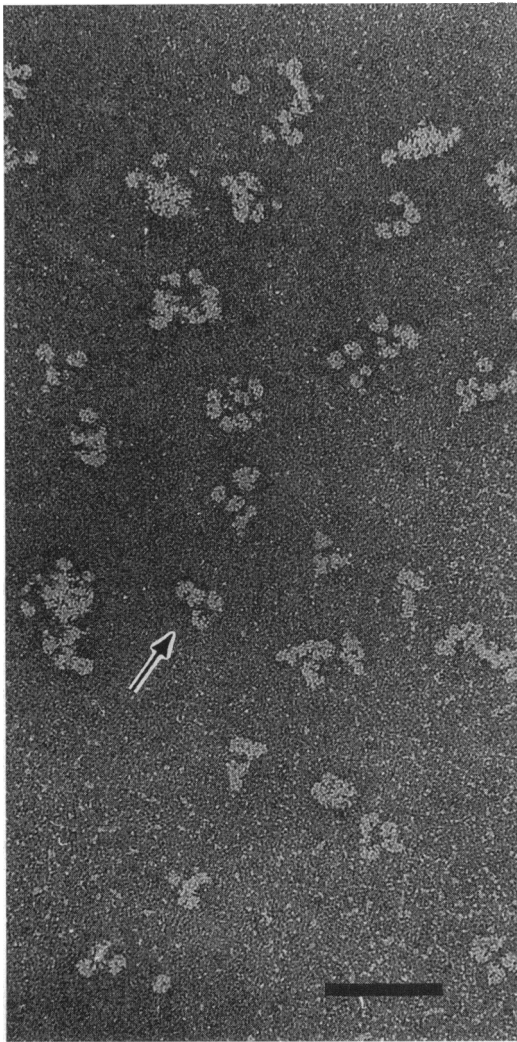


FIGURE 4 Negative stain of 22S dynein field prepared in parallel with dynein substrata used for translocation, but at 20 \times dilution. A three-headed 22S dynein molecule is indicated. Bar = 0.1 μm .

clusion also supports previous suggestions that the dynein interacts weakly with the overlying microtubule when not generating force.

Holwill et al. (1995) have developed a computer model to simulate our experiments. The initial simulation assumes that uniform nonstimulated control dynein is the substratum, that dynein arm activity is stochastic, and that the system behaves as though it were unloaded. The length of the microtubule sliding over the dynein substratum has been varied by varying the dynein arm density of the substratum—in this case a second microtubule in the simulation. For the times (~ 1 s) and microtubule lengths measured, the simulations are in quantitative agreement with our results in that a plot of v_0 versus L is hyperbolic in form, with severalfold scatter in the individual measurement at low values of L . Further work will test this model more rigorously. Although some variability in the measurement or sliding speed of microtubules of nearly the same length is

anticipated from the computer simulations, it is unclear whether the assumption of the simulations can account for all of the variability seen, for example, in the control dynein panel of Fig. 1 *a*. The variability does not seem to depend on sampling, because microtubules of similar length glide across the field at significantly different speeds when the sliding is observed in real time for over 1 min. Furthermore, tracings of the movement of individual microtubules of higher time resolution (100 ms), such as that presented in Hamasaki et al. (1995), show that, although microtubule sliding velocity is noisy, the microtubule does not stop. However, the few very slow microtubules moving at rates less than $0.5 \mu\text{m s}^{-1}$ have not been traced. One possible explanation for these slow velocities is that the cycle time (t_c) for a fraction of the individual unphosphorylated dynein molecules is very long. Whatever the reason, these microtubules represent a very small fraction of our measurements, and the remaining variation is of the same order as that measured by Uyeda et al. (1990) or Harris and Warshaw (1993) for myosin.

Based on a constant K_L of $4.1 \mu\text{m}$ at a density of 620 molecules μm^{-2} , the average $N(K_L)$ in our experiments is 60, provided that every dynein molecule in contact with the microtubule is functional. This also implies that one head of every molecule acts as the mechanochemical transducer. Because 22S dynein consists of three different heavy chains, each of which could perhaps propel the microtubule, $N(K_L)$ could be greater by a factor of up to 3. However, some 22S dynein molecules are likely to be oriented such that they approach the microtubule by an ATP-insensitive binding site or a nonbinding part of the molecule, and this will lead to an overestimate in $N(K_L)$. This is also true if some of the dyneins are dead heads. The overestimation is probably not greater than a factor of 2 in any case, because apparently dynein dead heads usually do not bind to the microtubule; also, tethered motors such as myosin or kinesin are functional in a wide range of attachment positions, and this seems likely to hold for dynein as well. Within the limitations of our data (Tables 1–3), we conclude that factors influencing the value of $N(K_L)$ do not change in any systematic way with dynein pretreatment.

In contrast to the randomly oriented nature of our preparations, the outer dynein arms on an intact subfiber A of a ciliary axonemal doublet microtubule are all oriented correctly to produce sliding, with 170 arms in $4.1 \mu\text{m}$. This linear density is, therefore, about three times (and perhaps as much as six times) greater than in the *in vitro* situation that we construct, which implies that the axonemal K_L for sliding is about 1 or 2 μm . Takahashi et al. (1982) showed that sliding of $\sim 30\text{-}\mu\text{m}$ -long doublet microtubules in axonemes proceeds at constant velocity for up to about 20 μm of elongation and tapers off only near the point where the sliding microtubules fall apart. This would be consistent with the estimated value of K_L for the axoneme.

Analytic interpretation of contributions of differently pretreated dyneins to v_o

Our results indicate that the maximum translocation velocity, v_o , varies with pretreatment, a conclusion that implies that the enzymatic properties of dynein vary with pretreatment, which in turn has significant implications for the mechanochemical parameters associated with the dynein-tubulin interaction. The treatments are of two types: one, detergent, changes the properties of nearly every dynein molecule in the field; the other, cAMP-induced phosphorylation, causes only a small percentage (less than 10%) of the dynein molecules (i.e., those with phosphorylated p29 (pp29) light chains) to have altered mechanochemical properties.

To interpret the results quantitatively, it is convenient to derive a relationship between the experimentally determined values for v_o associated with each form of dynein molecule. For control and detergent-treated preparations, the experimental values are those associated with the appropriate experimental form, because only one form is present. Where cAMP has been used to induce phosphorylation, two forms of molecular dynein contribute to the translocation, and the contribution of each one needs to be identified.

We have already concluded that the duty phase of the dynein activity cycle occupies on the order of 0.01 of the full cycle time, and that a microtubule of length K_L (4.1 μm) will touch about 60 dynein molecules. For such a microtubule, there is a probability of about 10% that two dynein molecules will interact simultaneously with the microtubule during a full cycle, but of less than 3% that three or more will so interact; this will have the effect of reducing the distance that a microtubule will move compared to that, D_t , predicted on the basis that all dynein molecules interact separately. Considering the situation for two dynein arms, the reduction will not be to 90% of D_t , because the duty phases will not be totally coincident but will usually overlap to some degree, on average by 50%. Accordingly, the distance moved will be about $0.95D_t$.

To make the analysis completely general, we shall assume that the three parameters associated with an active dynein molecule, namely the stepsize d^x , cycle time t_c^x , and duty phase t_s^x , are different for each form of the molecule, which is identified by the superscript x . Thus for control dynein $x = c$, for detergent-treated dynein $x = d$, and for cAMP-induced phosphorylated dynein $x = a$.

For a microtubule in contact with N dynein molecules, with a fraction p^x in form x , the distance D moved in time t is, approximately,

$$D = \sum_x \frac{t}{t_c^x} s^x p^x N d^x, \quad (8)$$

where s^x is to take account of the simultaneous activity of two molecules. We assume that the effect of simultaneous activity of two separate forms of dynein molecule is negli-

gible. In Eq. 8, the summation is over the forms of dynein molecule participating in the translocation, and, for the experiments considered here, will involve the four cases:

$$x = c; \quad x = c, a; \quad x = d; \quad x = d, a.$$

The microtubule velocity, v , that is measured experimentally after any pretreatment is given by

$$v = \frac{D}{t} = \sum_x s^x p^x N \frac{d^x}{t_c^x} = N \sum_x s^x p^x v_\alpha^x, \quad (9)$$

where v_α^x is the average velocity that would be induced by a single dynein molecule of type x acting alone on a microtubule. From Eq. (1),

$$v_\alpha^x = \frac{d^x}{t_s^x} = \frac{d^x}{t_c^x} \cdot \frac{t_c^x}{t_s^x} = \frac{v_\alpha^x}{f^x}. \quad (10)$$

From 9 and 10 we obtain

$$v = N \sum_x s^x p^x f^x v_\alpha^x. \quad (11)$$

The experimental values of microtubule sliding velocity v yield, from the derived hyperbola, the duty-phase velocity v_o , which is based on the implicit assumption that all of the dynein molecules are equivalent. In applying Eq. 11 to our results, we note that the value for s^x is essentially unity, whereas the constant value for K_L implies that f^x is constant for any x (Eq. 7). If we assume that both the proportion p^a and the maximum velocity v_o^a of phosphorylated dynein are the same with or without detergent treatment, Eq. 11 allows us to form two simultaneous equations, from which these parameters may be determined. Using the data from Table 4, we obtain a value of $10.4 \mu\text{m s}^{-1}$ for v_o^a and of 14% for the proportion of phosphorylated dynein in the two preparations. This proportion is only slightly higher than the 2–10% that can be estimated from the experimental procedures. Alternatively, it may be that the detergent affects the maximum velocity associated with the phosphorylated dynein, or that the proportion of phosphorylated dynein molecules is not the same in the two cases, or that both parameters are different in the two situations. Our results are not sufficiently precise to eliminate these alternative assumptions, but considering the first (and most likely) of these possibilities, and taking a value of 10% for the proportion of phosphorylated dynein present in the experiments, we calculate v_o^a to be $13.7 \mu\text{m s}^{-1}$. For the detergent-treated samples, $v_o^{a,d}$ is $12.8 \mu\text{m s}^{-1}$, which might mean that detergent actually slows the speed at which a phosphorylated dynein can push.

Taking 2% as the proportion of phosphorylated dynein, we calculate v_o^a to be $57.4 \mu\text{m s}^{-1}$ and $v_o^{a,d}$ to be $45.0 \mu\text{m s}^{-1}$. These values are probably too high to be correct, which suggests that the proportion of phosphorylated dynein after cAMP treatment is closer to 10% than to 2%.

When the two treatments are applied together, the velocity increases above that obtained by treatments with cAMP

or detergent alone (Table 4), which is consistent with an additional effect of a small number of experimentally phosphorylated p29 (pp29) imposed on the more global effect of detergent. It seems likely that Triton would affect hydrophobic interactions in 22S dynein, perhaps changing the head-head distance or the relationships of various other subcomponents of the molecule slightly, whereas pp29 probably has a specific effect on the charge distribution around its binding site on the α heavy chain. Within the limitations discussed here, K_L is not affected by Triton, which implies that no additional molecules are activated by the detergent, and probably means that changes in ATPase activity (Gibbons and Fronk, 1979) and v_o^* cannot be accounted for by changes in the numbers of globular heads that produce sliding, but rather by changes in some properties of the heads themselves.

If 2–10% of the p29 is experimentally phosphorylated, a K_L microtubule length of 4.1 μm will normally encounter some 1–6 dyneins with pp29. One consequence of this may be that, as we demonstrate, a field of detergent-treated dynein will have a higher v_o^* than the field of dynein with pp29, even if the alterations in mechanochemistry caused a more significant increase in velocity in the latter instance. A second consequence is that microtubules will glide over variable small numbers of pp29 dyneins in the experimentally phosphorylated substrata during short measurement times; thus, a given microtubule may speed up significantly in velocity measured over short times, as we have sometimes observed (Hamasaki et al., 1995).

From Eq. 10, a change in v_o^* implies a change in step size (d^x), cycle time (t_c^x), or f^x . A constant f^x implies that an increase in v_o^* by p29 phosphorylation would require either an increase in step size by the affected molecule or a decrease in cycle time or both changes. However, if f^x is a constant, a change in overall cycle time would imply that t_s^x would also change. An alternative assumption, consistent with the range of values we measure, would be that as v_o changes, t_s remains constant because of compensating changes in f and t_c . Direct kinetic measurements of the mechanochemical cycle steps that might permit us to decide between these alternatives are not yet available.

Relation to beat frequency

Studying the beat frequency of mussel gill lateral cilia as a function of serotonin (5HT) concentration, Sanderson et al. (1985) found that frequency increased approximately linearly from 0 to 20 Hz over the range of 10^{-9} to 10^{-5} M 5HT. In these cilia, 5HT apparently activates adenylyl cyclase, causing an increase in intracellular cAMP (Scheide and Dietz, 1984). An increase in beat frequency is seen in permeabilized lateral cilia when they are perfused with cAMP (Murakami, 1987), precisely as in *Paramecium*. These studies suggest that over most, if not all, of the physiological range of beat frequency, in other organisms as well as in *Paramecium*, the velocity of microtubule sliding

increases in proportion to the percentage of cAMP-dependent phosphorylation of p29 or its homolog.

Estimates of the time (t_E , Table 4) for development of a bend of 100° , a typical effective stroke displacement for a vertically standing cilium, and one that involves interdoubtlet sliding of about 0.1 μm , are about one-quarter of the beat period. For any given velocity of in vitro microtubule sliding, it is then possible to calculate a corresponding ciliary beat frequency (H), variations in which reflect the alterations in the mechanochemical parameters of the 22S outer arm dynein. Frequencies estimated in this way for a number of different pretreatment conditions are shown in Table 4, where

$$v_o^* = 0.4 H \quad (12)$$

In control 22S dynein, p29 is probably partially phosphorylated, corresponding to a beat frequency of 6.7 Hz (Table 4). The small percentage increase in p29 phosphorylation associated with cAMP pretreatment would produce a corresponding small increase in beat frequency within the physiological range, similar to that expected by a ~ 4 -fold increase in stimulus intensity, based on the Sanderson et al. (1985) data. Our calculations in the previous section suggest that complete phosphorylation of all p29 would lead to a v_o^* of 10.4 $\mu\text{m s}^{-1}$ to 57.4 $\mu\text{m s}^{-1}$, i.e., consistent with the range for maximal velocity of sliding microtubules determined for disintegrating axonemes (V_{max} of Takahashi et al., 1982) and a beat frequency of ≥ 26 Hz. However, the data of Takahashi et al. (1982) may come from axonemes that have not been maximally stimulated. One additional calculation possible from these data is $2.5 d/t_{c \text{ max}}$ (Table 4), the theoretical maximum beat frequency based on a maximum step size and a minimum cycle time for the 22S molecule. Estimates of minimal cycle times (33 ms) from kinetic data, i.e., a rate-limiting step of 6 s^{-1} for ADP release coupled with a 5-fold activation of rate in the presence of microtubules (Omoto and Johnson, 1986), and of maximal outer arm step size (16 nm) from geometrical considerations (Satir et al., 1981), have been obtained. Other workers have suggested maximum step sizes of up to 40 nm (Brokaw, 1975; Oiwa and Takahashi, 1988). For $d = 16$, $t_c = 33$, this calculation yields a value of about 120 Hz, on the order of the highest beat frequencies measured. Because the majority of ciliates and flagellates have organelle beat frequencies in the range 5 to 60 Hz, the mechanochemical system operates well within its limitations. This value also suggests that our calculation of the upper limit of v_o^* (Table 4) is too high.

Taken together, these types of calculations suggest that the mechanochemical parameters of 22S dynein can be altered in several ways to increase microtubule sliding velocity and beat frequency. In physiological situations, these alterations may be caused by an increase in the numbers of dynein molecules with pp29 or a corresponding homolog, which, with an initial stimulus, decrease their cycle time and then, under greater stimulation, increase step size to bring

about faster microtubule sliding velocities, and hence beat frequencies, under cellular control, until an upper limit is reached. The results of microtubule translocation experiments in this paper have been used to infer detailed temporal and spatial characteristics associated with the dynein arm cycle under a range of in vitro conditions. Although we have indicated how this may relate to the behavior of dynein arms in the living axoneme, and particularly to the increase in beat frequency seen upon stimulation in ciliated cells, both the mechanochemical and the physiological implications of the quantitative relationships developed here clearly require further testing.

We thank Steven M. Block, Jeffrey E. Segall, and Allan W. Wolkoff for helpful advice.

This work was supported in part by grants from the National Institutes of Health (RR 09785) to P.S. and the United Kingdom Biotechnology and Biological Sciences Research Council (GR J34002) to M.E.J.H., and from NATO (CRG 930141) for International Collaboration in Research. T.H. was a postdoctoral fellow of the American Heart Association (New York Affiliate); K.B. was a graduate fellow supported by National Institutes of Health training grant CA09475.

REFERENCES

Barkalow, K., J. Avolio, M. E. J. Holwill, T. Hamasaki, and P. Satir. 1994a. Structural and geometrical constraints on the outer dynein arm in situ. *Cell Motil. Cytoskel.* 27:299–312.

Barkalow, K., T. Hamasaki, and P. Satir. 1994b. Regulation of 22S dynein by a 29 kDa light chain. *J. Cell Biol.* 126:727–735.

Block, S. M., L. S. B. Goldstein, and B. J. Schnapp. 1990. Bead movement by single kinesin molecules studied with optical tweezers. *Nature.* 348:348–352.

Briggs, G. E., and J. B. S. Haldane. 1925. A note on the kinetics of enzyme action. *Biochem. J.* 19:338–339.

Brokaw, C. J. 1967. Adenosine triphosphate usage by flagella. *Science.* 156:76–78.

Brokaw, C. J. 1975. Cross-bridge behavior in a sliding filament model for flagella. In *Molecules and Cell Movement*. S. Inoue and R. Stephens, editors. Raven Press, New York. 165–179.

Finer, J. T., R. M. Simmons, and J. A. Spudich. 1994. Single myosin molecule mechanics: piconewton forces and nanometre steps. *Nature.* 368:113–119.

Gibbons, I. R., and E. Fronk. 1979. A latent adenosine triphosphatase form of dynein-1 from sea urchin sperm flagella. *J. Biol. Chem.* 254:187–196.

Hamasaki, T., K. Barkalow, J. Richmond, and P. Satir. 1991. A cAMP-stimulated phosphorylation of an axonemal polypeptide that copurifies with the 22S dynein arm regulates microtubule translocation velocity and swimming speed in *Paramecium*. *Proc. Natl. Acad. Sci. USA.* 88:7918–7922.

Hamasaki, T., I. Simon, K. Barkalow, and P. Satir. 1995. Activation of dynein-mediated microtubule translocation via phosphorylation of a 29 kDa light chain. *Biophys. J.* 68:323s.

Harada, Y., K. Sakurada, T. Aoki, D. D. Thomas, and T. Yanagida. 1990. Mechanochemical coupling in actomyosin energy transduction studied by in vitro movement assay. *J. Mol. Biol.* 216:49–68.

Harris, D., and D. M. Warshaw. 1993. Smooth and skeletal muscle myosin both exhibit low duty cycles at zero load in vitro. *J. Biol. Chem.* 268:14764–14768.

Holwill, M. E. J., G. F. Foster, T. Hamasaki, and P. Satir. 1995. Biophysical aspects and modelling of ciliary motility. *Cell Motil. Cytoskel.* 32:114–120.

Howard, J., A. J. Hudspeth, and R. D. Vale. 1989. Movement of microtubules by single kinesin molecules. *Nature.* 342:154–158.

Hunt, A. J., F. Gittes, and J. Howard. 1994. The force exerted by a single kinesin molecule against a viscous load. *Biophys. J.* 67:766–781.

Johnson, K. A. 1985. Pathway of the microtubule-dynein ATPase and the structure of dynein: a comparison with actomyosin. *Annu. Rev. Biophys. Chem.* 14:161–188.

Lineweaver, H., and D. Burk. 1934. The determination of enzyme dissociation constants. *J. Am. Chem. Soc.* 56:658–666.

Murakami, A. 1987. Control of ciliary beat frequency in the gill of *Mytilus*. I. Activation of the lateral cilia by cyclic AMP. *Comp. Biochem. Physiol.* 86C:273–279.

Oiwa, K., and K. Takahashi. 1988. The force-velocity relationship for microtubule sliding in demembrated sperm flagella of the sea urchin. *Cell Struct. Func.* 13:193–205.

Omoto, C. K., and K. A. Johnson. 1986. Activation of the dynein adenosine triphosphatase by microtubules. *Biochemistry.* 25:419–427.

Press, W. H., S. A. Teukolsky, W. T. Vetterling, and B. P. Flannery. 1992. *Numerical Recipes in C*, 2nd ed. Cambridge University Press, New York. 683–688.

Sanderson, M. J., E. R. Dirksen, and P. Satir. 1985. The antagonistic effects of 5-hydroxytryptamine and methylxanthine on the gill cilia of *Mytilus edulis*. *Cell Motil.* 5:293–309.

Satir, P., K. Barkalow, and T. Hamasaki. 1993. The control of ciliary beat frequency. *Trends Cell Biol.* 3:409–412.

Satir, P., J. Wais-Steider, S. Lebduska, A. Nasr, and J. Avolio. 1981. The mechanochemical cycle of the dynein arm. *Cell Motil.* 1:303–327.

Scheide, J. I., and T. H. Dietz. 1984. The effects of calcium on serotonin-stimulated adenylate cyclase in freshwater mussels. *Biol. Bull.* 166:594–607.

Svoboda, K., C. F. Schmidt, B. J. Schnapp, and S. M. Block. 1993. Direct observation of kinesin stepping by optical trapping interferometry. *Nature.* 365:721–727.

Takahashi, K., C. Shingyoji, and S. Kamimura. 1982. Microtubule sliding in reactivated flagella. *Symp. Soc. Exp. Biol.* 35:159–177.

Uyeda, T. Q. P., S. J. Kron, and J. A. Spudich. 1990. Myosin step size. Estimation from slow sliding movement of actin over low densities of heavy meromyosin. *J. Mol. Biol.* 214:699–710.

Vale, R. D., F. Malik, and D. Brown. 1992. Directional instability of microtubule transport in the presence of kinesin and dynein, two opposite polarity motors. *J. Cell Biol.* 119:1589–1596.

Vale, R. D., and Y. Y. Toyoshima. 1988. Rotation and translocation of microtubules in vitro induced by dyneins in *Tetrahymena* cilia. *Cell.* 52:459–469.

Vale, R. D., and Y. Y. Toyoshima. 1989. Microtubule transduction properties of intact and proteolytically digested dyneins from *Tetrahymena* cilia. *J. Cell Biol.* 108:2327–2334.

Walczak, C. E., and D. L. Nelson. 1994. Regulation of dynein-driven motility in cilia and flagella. *Cell Motil. Cytoskel.* 27:101–107.

Yanagida, T., Y. Harada, and A. Ishijima. 1993. Nano-manipulation of actomyosin molecular motors in vitro: a new working principle. *Trends Biochem. Sci.* 18:319–324.